

1 **Developing a High-resolution Emission Inventory Tool for Low-Carbon City**
2 **Management Using Hybrid Method – A Pilot Test in High-density Hong Kong**

3 Meng CAI ^a, Yuan SHI ^b, Chao REN ^{c*},

4 ^a School of Architecture, The Chinese University of Hong Kong

5 ^b Institute of Future Cities, The Chinese University of Hong Kong

6 ^c Faculty of Architecture, The University of Hong Kong

7

8 *The corresponding author's email addresses: renchao@hku.hk

9

10 **Highlights**

- 11 • A hybrid method was developed to model urban carbon emission at high-resolution.
- 12 • Open urban form data of building attributes and traffic flow were utilized.
- 13 • The hybrid method was demonstrated in high-density Hong Kong.
- 14 • Annual carbon emission maps were generated for the building and transport sectors.
- 15 • Validation results show the robustness and broad applicability of the method.

16

17 **Abstract**

18 Energy is one of the crucial elements in creating resilience in cities. Global cities produce more
19 than 70% of the world's carbon emissions from energy activities and thus play an important role
20 in changing climate and causing environmental problems. The spatial modelling of urban carbon
21 emissions can serve as the basis for carbon emissions mitigation. Building attributes are the key
22 energy demand indicators and significant in constructing the emission inventory, but they are often

23 not accounted for in the modelling process due to data availability. Therefore, this study aims to
24 develop a tool for modelling a high-resolution emission inventory using open urban form data and
25 demonstrate it for Hong Kong. This tool modelled the urban carbon emissions for building and
26 transport sectors using a hybrid method involving both bottom-up and top-down approach. Open
27 urban data including building attributes and traffic flow were extracted as model input data. The
28 urban carbon emissions were modelled for Hong Kong at 100m spatial resolution for different
29 sectors and integrated in Tertiary Planning Unit. Validation results show that the method has
30 reasonably represented both the total emissions and the spatial pattern of urban carbon emissions
31 of Hong Kong. The spatial distribution of carbon emissions of Hong Kong can provide reference
32 information for low-carbon city management for other high-density cities. The method shows the
33 potentially broad applicability, therefore contributing to the global collaborative effort in the
34 mitigation of carbon emissions.

35
36 **Keywords:** high-resolution emission inventory, urban carbon emissions, low-carbon city, urban
37 form, open data.

38 39 1. INTRODUCTION

40 Climate change has caused a series of effects on Earth, such as rising temperatures and sea levels
41 [1]. The anthropogenic climate change primarily results from the combustion of fossil fuels, which
42 produce greenhouse gas (GHG) emissions. The Intergovernmental Panel on Climate Change
43 (IPCC) further stressed that carbon dioxide (CO₂) is the most important anthropogenic GHG in
44 2007 [2]. Energy is one of the crucial elements in creating resilience in cities because it is
45 indispensable in sustaining citizens, diverse urban functions, industry and the overall economic
46 growth of cities [3]. Cities account for about 64 percent of global primary energy use and produce

47 over 70 percent of carbon emissions from energy activities [1, 4]. Thus, cities are the main targets
48 for reducing carbon emissions. The United Nations estimate that the major increase of the global
49 population will happen in cities from 2012 to 2050 [5]. World carbon emissions are expected to
50 increase due to continuous urbanization.

51

52 Urban carbon emissions inventories can provide the basis for reducing carbon emissions and
53 low-carbon development [6]. However, national or citywide estimations of carbon emissions are
54 still the major source for informing the policymaking process, which is insufficient for the
55 formation of the carbon emissions mitigation strategies [7]. Due to the absence of detailed
56 information on spatial distributions, the spatial carbon emission dynamics within an
57 administrative unit such as city or community boundary have not been clarified. Thus, it is
58 necessary to develop finer-scale carbon emission inventories [7].

59

60 There are two commonly used methods for the spatial modelling of carbon emissions: 1) bottom-
61 up analyses, a method that involves accurate emission data from sectoral energy consumption
62 data [8] or point source carbon emission data [9]; 2) top-down models that distribute the carbon
63 emissions of a large area to finer spatial unit based on certain proxy data and algorithms. The
64 bottom-up method generally calculated the carbon emissions from the emission sources and can
65 achieve the most accurate results [9, 10]. There are some open carbon emission products derived
66 from the bottom-up method at global or national scale developed by government authorities or
67 the planning departments, such as China High Resolution Emission Database (CHRED)[10] ,
68 Emission database for global atmospheric research (EDGAR) [11], Vulcan in the United States

69 [12]. Despite the good spatial coverage, these datasets have coarse spatial resolution larger than
70 1km which does not provide enough detailed information on the spatial patterns of carbon
71 emissions within an administrative unit. Apart from these publicly available datasets at the
72 national or the global scale, many urban carbon modelling studies have been conducted for
73 individual cities to achieve more detailed and localized data to better inform the local low-carbon
74 strategies [9, 13-15]. However, the workflows developed by the above studies cannot be widely
75 applied to global cities due to the lack of detailed urban data. As a result, the comparability and
76 applicability of these studies are limited since it is insufficient to estimate carbon emissions
77 distribution for different cities [16].

78

79 The top-down method using proxy data to disaggregate the statistical carbon emissions to a
80 certain spatial unit is based on the assumption that the proxy data is correlated with the carbon
81 emissions related to the energy consumption of the same pixel [17]. The Nightlight (NTL) data
82 population data, and land use data have been extensively used as the proxy data since they can
83 provide a proper estimation of the human activities and socioeconomic conditions [18-22] [23].

84 The top-down method using these datasets can be easily implemented using openly available
85 data for a large study area. However, the NTL data have saturation problem and cannot fully
86 represent emissions from the transport and industrial sectors [24]. The population data cannot
87 reflect some potential emissions in the commercial and industrial sectors without human
88 settlement [25]. In addition, demographics cannot be used to pinpoint the exact location of
89 emission sources since the census data usually indicate statistics at the administrative level or
90 within a large spatial grid [25]. Also, the land use information can only provide a general
91 characterization of the energy demand. Furthermore, the NTL, population data and land use data

92 cannot reflect the variations of carbon emissions across different buildings. Meanwhile, building
93 attributes are the key energy demand indicators and have also been applied in the top-down
94 models [26]. In comparison with the nightlight and population data, the building information can
95 reflect the energy performance in the business and industrial sectors and can highlight the
96 location of the emission sources. Moreover, it is necessary to account for the building emissions
97 since the building sectors are the major contributors to urban carbon emissions, especially for
98 cities under rapid urbanization [27]. However, it is found that most studies on urban carbon
99 emissions in China did not account for the building data due to data availability [28]. It is
100 necessary to involve building data for a comprehensive and accurate top-down model of the
101 spatial inventory of urban carbon emissions.

102

103 In sum, the previous spatial urban carbon emission inventories often have a coarse spatial
104 resolution greater than 500m. Moreover, building information is found to have an impact on carbon
105 emissions in urban areas [29-31]. A more accurate spatial pattern of urban carbon emissions can
106 be modelled by incorporating building data. However, high-quality building data are often missing
107 or not publicly available. Thus, there is still no universally applicable tool to model urban carbon
108 emissions for different cities [32]. The openness and availability of urban carbon emissions data
109 directly affect scientific research, the formation of low-carbon strategies and public participation
110 in climate change mitigation [9, 33, 34].

111

112 Thus, it is necessary to develop a method for modelling carbon emissions spatial inventories at a
113 finer resolution using publicly available urban form dataset. A consistent methodology using
114 publicly available urban form data is essential for a better global collaborative effort in urban

115 resilience and carbon emission mitigation. The spatial modelling of carbon emissions can serve as
116 the foundation for the city 's carbon emission inventory and help to evaluate practical measures
117 for the development of low-carbon cities to mitigate climate change. To fulfill the above needs, in
118 this study, we develop an approach to model high-resolution carbon emission inventories and
119 demonstrate the approach through implementation in Hong Kong, a city with high-density urban
120 context and rising urban carbon emissions [35].

121

122 **2. MATERIALS AND METHODS**

123

124

125 **2.1 Study area and data**

126

127 Hong Kong is one of the most high-density cities in the world, with population of more than 7
128 million people and land area of 1,100 square kilometres [36]. With population growth and
129 economic development, Hong Kong's energy consumption has increased significantly in the past
130 few decades [37, 38]. Massive GHG was produced from energy usage in Hong Kong. In 2016,
131 the GHG emissions were 41.09 million tons (Mt), of which about 90% were generated from energy
132 activities [37]. From 1990 to 2013, per capita carbon emissions increased from 6.031 tons per
133 capita to 7.225 tons per capita[35]. The impacts of climate change such as rising temperatures,
134 frequent occurrences of extreme weather events and rising sea levels, have already affected Hong
135 Kong [39]. The local government has set a target to reduce carbon intensity, i.e. the carbon
136 emissions per unit GDP, to 65% -70% of the intensity in 2005 by 2030 for the development of the
137 low-carbon city [38].

138

139 Moreover, high-rise buildings are compactly distributed in the urban areas in Hong Kong [40].
140 Compared with other emission sources in Hong Kong, buildings produce the largest amount of
141 carbon emissions [39]. Therefore, it is necessary to mitigate the emissions from the buildings and
142 account for building attributes in the spatial modelling of carbon emissions [39].



143
144 Fig. 1. 18 districts of Hong Kong [36]

145
146 The study involves statistical data, spatial data, and emission parameters. Statistical data on fossil
147 fuel consumption in Hong Kong including the Hong Kong energy statistic reports and Hong Kong
148 energy end-use report only include energy consumption data counted at the city-level [37, 41]. The
149 emission parameters were collected from IPCC [42]. The spatial data were adopted as the emission
150 source and the proxy. There are mainly four types of transportation in Hong Kong: road network,
151 Mass Transit Railway (MTR), civil aviation and marine. Therefore, the spatial data for the
152 transport sector include road traffic flow and MTR route from the transportation department, civil
153 aviation emissions from the civil aviation department, marine emissions [37]. The spatial data were

154 all converted to raster format with 100m grid size. All the statistical and spatial data of 2016 were
 155 acquired for the consideration of data integrity.

156 Table 1. input data for the carbon emission model

Category	name	source	Reference
Statistical data	Hong Kong Energy Statistics	Census and Statistics Department	[41]
	Hong Kong energy end-use report	Electrical & Mechanical Services Department of Hong Kong (EMSD)	[37]
	Civil aviation emissions	Civil aviation department	[43]
Specific coefficients	CO2 Emission factors	IPCC	[42]
	Oxygenation efficiency	IPCC	[42]
	Net calorific Values	IPCC	[42]
spatial data	TPU boundary	Census and Statistics Department	https://www.census2011.gov.hk/en/tertiary-planning-units.html
	Traffic volume	Transportation department	[44]
	MTR route	MTR Corporation Limited	https://data.gov.hk/en-data/dataset/mtr-data-routes-fares-barrier-free-facilities/resource/31c59d00-11b0-4f67-b7c8-5721f0e4addf
	Ferry	Transportation department	https://data.gov.hk/en-data/dataset/hk-td-tis_14-routes-fares-xml/resource/521c1303-7318-4f0a-b60c-00a82269a1a1
	3D building	Google maps and AW3D30	[45]
	Building use	Data.gov.hk, Hong Kong Geodata store, Google maps, Amap	To be elaborated in table 2

158 **2.2 Model description**

159 In this study, a hybrid model involving both top-down and bottom-up methods was applied. Four
160 sectors (transport, business, industry, and residence) will be accounted for in this model. We
161 account for energy-related emissions including direct emissions from fossil fuels as well as indirect
162 emissions from heating and power generation for each sector.

163
164 Firstly, the total emissions in each sector will be calculated following the IPCC guidelines (IPCC,
165 2006). The emissions that have specific spatial information and can be directly derived from
166 openly available sources such as civil aviation, marine, will be modelled using the bottom-up
167 method that directly assigns the emissions to the spatial grid of the emission source.

168
169 For emissions without detailed spatial information or publicly available sources, the spatial
170 distribution of the carbon emissions can be modelled by the top-down method that distributes the
171 statistical data to the emission source using proxy data. For building emissions including the
172 business, industrial and residential sectors, buildings are considered as the emission source.
173 Building attributes are identified as key energy performance indicators and form the basis of the
174 building typology categorization [26]. Building attributes relevant to energy consumption include
175 building use, as well as morphological attributes such as building volume, window, wall and roof
176 areas [26]. The building volume density (BVD) represents the building morphology and provides
177 an estimate of the space of the building [45]. The integration of BVD and building use can be used
178 to assign the energy demand and thus is key in quantifying building carbon emissions. Therefore,
179 building attributes including the building use and the BVD will be used as proxy data for allocating
180 the emissions from buildings.

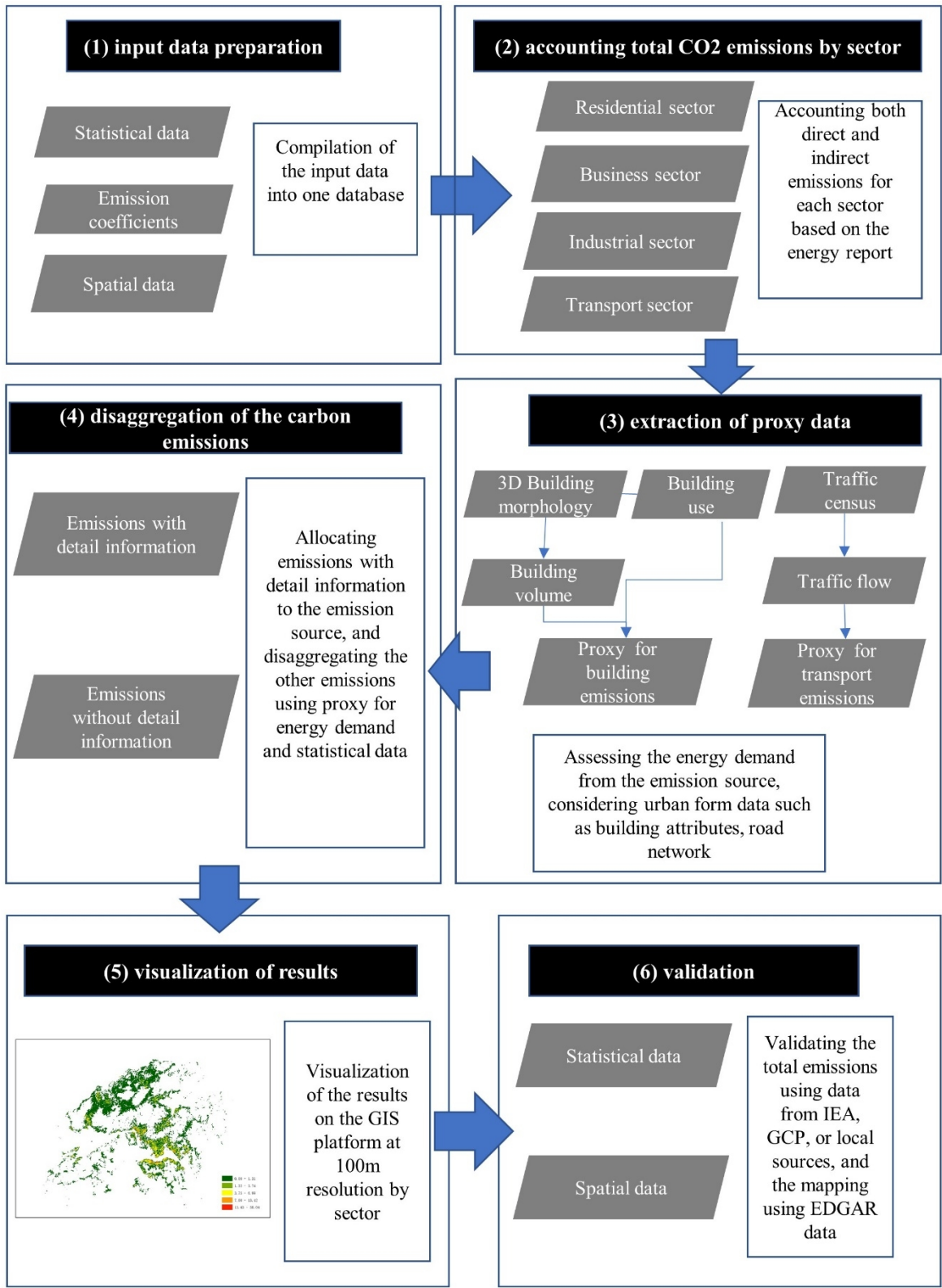
181

182 For the transport sector, the road network is regarded as the emission source. Traffic flow is the
183 product of traffic density and velocity, so the traffic flow along the road network can reflect the
184 patterns of traffic emissions [46]. Traffic flow will be modelled and be used as a proxy to calculate
185 the transport emissions. Therefore, the emissions from each sector can be modelled and visualized
186 on the Geographical Information System (GIS) platform. Finally, the statistical and spatial
187 modelling results will be validated by other publicly available datasets.

188

189 Therefore, the model for creating the inventory contains six steps (Fig. 2): (1) preparation of input
190 data; (2) accounting total carbon emissions by sector; (3) extraction of proxy data, including
191 building use, building morphology and traffic flow; (4) disaggregation of the statistical data on
192 carbon emissions to the level of emission sources; (5) visualization of results; (6) valuation of the
193 results. The procedure will be illustrated with more details in section 2.3.

194



195

196

Fig. 2. the procedure for developing a spatial carbon inventory

197 **2.3 Model application in Hong Kong**

198 **2.3.1 accounting total CO2 emissions by sector**

199 The urban carbon emissions in Hong Kong include the emissions from the residential, business,
200 industrial and transport sector. The emissions consist of direct emissions from fossil fuel
201 combustion and indirect emissions from electricity generation. Hong Kong has a monsoon-
202 influenced subtropical climate with warm winter, so the indirect emissions mainly come from
203 electricity generation and the emissions from heat production can be neglected. Following the
204 method in the IPCC report [42], the fossil fuel-related emissions were calculated as:

$$205 \quad CE_{ij} = AD_{ij} \times NCV_j \times EF_j \times O_{ij} \quad (1)$$

206 where i presents different sectors, j shows fossil fuels type. CE_{ij} indicates the carbon emissions by
207 sector i and fossil fuels type j . AD_{ij} denotes fossil fuel consumption. NCV , EF , and O are emission
208 parameters of different fossil fuel types, which represent net caloric value, emission factors, and
209 the oxygenation efficiency, respectively.

210

211 The indirect emissions were calculated based on primary energy input from Hong Kong Energy
212 Statistics:

$$213 \quad CE_i = CE \times \frac{E_i}{E} \quad (2)$$

214 where CE is the total emissions from electricity generation, E_i represents the electricity
215 consumption by sector i . Therefore, the carbon emissions for each sector can be acquired by
216 aggregating the direct and indirect emissions.

217

218

219

220 **2.3.2 spatial mapping of carbon emissions in the building sector**

221 **a). extraction of building use**

222 The building attributes including the building use and building morphology will be extracted from
223 open data to spatially model the urban carbon emissions in Hong Kong. According to the Hong
224 Kong energy end-use report (Electrical & Mechanical Services Department of Hong Kong, 2018),
225 there are statistics of energy consumption of different building uses in each sector, which is helpful
226 to disaggregate the carbon emissions in each sector in more details. There are nine building use
227 types from the report (Table 2). For the building use of the retail, office, accommodation, health
228 and education, the name lists of the buildings have been provided by the local government
229 (Data.gov.hk). The name lists were converted to the geographical coordinates using the geocoding
230 function of the Google JavaScript Application programming interface (API). The housing
231 authority (HA) of Hong Kong provided the name list of the public housing and the HA subsidized
232 sale flats. The name lists were also converted to the geographical coordinates using Geocoding.
233 The location information of the private housings which is unavailable from the local government
234 was extracted using the Web scraping from Amap.com. All the building use data were converted
235 to point type in the GIS format based on the extracted coordinates.

236

237 Table 2. sources to extract building use types in Hong Kong

Sector	Building use	Source	Local or global	Link
business	Retail	Data.gov.hk	Local	https://data.gov.hk/en-data/dataset/rehabsociety-access-accessible-

				facilities/resource/44bd093c-756b-4c1e-b2f7-a8674503ff89
	Office	Data.gov.hk	Local	https://data.gov.hk/en-data/dataset/hk-landsd-openmap-geo-referenced-public-facility-data
	Accommodation	Data.gov.hk	Local	https://data.gov.hk/en-data/dataset/hk-had-json1-licensed-hotels-and-guesthouses
	Health	Data.gov.hk	Local	https://data.gov.hk/en-data/dataset/hospital-hadata-health-care-facilities
	Education	Data.gov.hk	Local	https://data.gov.hk/en-data/dataset/hk-edb-schinfo-school-location-and-information
	Restaurant	Data.gov.hk	Local	https://data.gov.hk/en-data/dataset/rehabsociety-access-accessibile-facilities/resource/44bd093c-756b-4c1e-b2f7-a8674503ff89
Residential	Public housing	Housing authority	Local	https://www.housingauthority.gov.hk/en/global-elements/estate-locator/index.html
	Private housing	Web scaping from Amap.com	global	

	HA subsidized	Housing	Local	https://www.housingauthority.gov.hk/en/global-elements/estate-locator/index.html
	sale flats	authority		
Industrial	factories	Housing	Local	https://www.housingauthority.gov.hk/en/global-elements/estate-locator/index.html
		authority		

238

239 **b). extraction of building morphology**

240 Building morphology was obtained by a simple and efficient approach using open data [45]. The
 241 Maps Static application programming interface (API) was used to extract the building footprints
 242 and the building heights were generated from a free digital surface model named the ALOS World
 243 3D model with a resolution of 30 m (AW3D30). A spatial join was then applied in GIS between
 244 the extracted points of building use and the extracted building to assign the building use attributes.

245

246 Thereafter, the building footprints and building heights were used to calculate the BVD for each
 247 building use. The BVD is determined by the total building volume divided by the land area:

248
$$BVD = \frac{\sum_{i=1}^N (C_i \times h_i)}{S_L} \quad (1)$$

249 where i is the building on the land area, C means the area of building, h represents the building
 250 height and S_L is the land area size. The land area was determined as 100m.

251

252 **c). building emissions mapping**

253 The total emissions from buildings (industrial, business and residential sectors) were further
 254 refined as the emissions from each building use, based on the percentage of the energy

255 consumption of each building use in each sector. Thereafter, the emissions from each building use
256 were proportionally assigned to each building based on the BVD for each building use. Therefore,
257 the building carbon emissions of a certain pixel p can be calculated as:

$$CE_p = CE_i \times \frac{E_j}{E_i} \times \frac{BVD_p}{\sum BVD_j} \quad (4)$$

258 where i and j represent the sector and the building use in the sector for the pixel p , respectively.
259 E means energy consumption. BVD_p is the BVD value for the pixel p and the $\sum BVD_j$ is the total
260 BVD value for the building use j .

261

262 **2.3.3 spatial mapping of carbon emissions in the transport sector**

263 **a). traffic flow estimation**

264 The Hong Kong transportation data released by the Hong Kong Transport Department were used
265 to simulate the traffic flow on the road network. In the Annual Traffic Census 2016, the annual
266 average daily traffic (A.A.D.T.) of 1662 counting stations in Hong Kong were surveyed. In this
267 study, we used the Lagrangian model proposed by Xia and Shao [46] to simulate traffic flow on a
268 complex road network based on the A.A.D.T.. This simple method will be quite efficient if there
269 is sufficient road network data.

270

271 **b). transport emissions mapping**

272 Transportation emissions from fossil fuels mainly consist of road traffic emissions, civil aviation
273 emissions, and marine emissions. The civil aviation emissions and marine emissions were
274 calculated based on the data from the civil aviation department and Hong Kong energy end-use
275 report [37], respectively. Therefore, the emissions from civil aviation and marine were directly

276 assigned to the geographical location of the airport and the ferries. The indirect emissions in the
277 transport sector are the emissions from the MTR. So, the transportation emissions from electricity
278 were equally assigned to the rasterized grid of the MTR route. Emissions from the road network
279 were calculated by excluding the marine, civil aviation and MTR emissions from the total transport
280 emissions. The road network emissions were distributed to the spatial grid of the road network
281 based on the proportion of the traffic flow.

282

283

284 The total urban carbon emissions were mapped out by aggregating the emissions from different
285 sectors. The emissions were finally averaged in each Tertiary Planning Unit (TPU) of Hong Kong
286 for further planning recommendation. TPU was designed for town planning purpose and there are
287 total 291 TPUs in Hong Kong.

288

289 **3. RESULTS AND VALIDATION**

290 **3.1 Total carbon emissions**

291 The total emissions were 42.09 Mt in 2016, which is closed to the emissions (41.7 Mt) published
292 by Environmental Protection Department of Hong Kong [35], and the emissions from the global
293 carbon project (43 Mt). 33.55 Mt emissions are from buildings (residential, business and industrial
294 sector), and 8.54 Mt from the transport sector. Buildings are the major contributors to carbon
295 emissions and produce over 80% of the entire emissions. Buildings are also identified to consume
296 more than 90 percent of the electric power. 19% of the emissions come from Oil & coal products,
297 which are mainly consumed in the transport sector. TownGas & LPG contributed to the least
298 carbon emissions among all fossil fuel types.

299

300

301

302 Table 3. Total carbon emissions by sector (Mt)

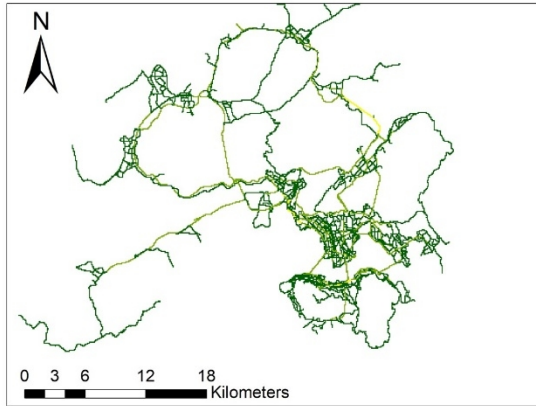
Sector	Oil & coal products	TownGas & LPG	Electricity	Total
residential	0.00	1.15	8.50	9.65
business	0.47	0.93	20.47	21.87
industrial	0.39	0.06	1.57	2.03
transport	6.97	0.93	0.63	8.54
Total	7.84	3.08	31.18	42.09

303

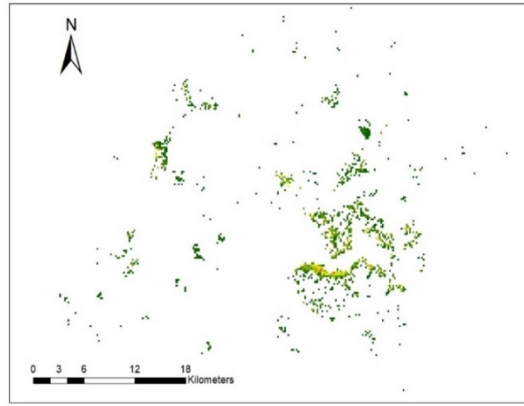
304 3.2 Spatial distribution of urban carbon emissions

305 The emissions from different sectors as well as the total emissions were mapped out on a 100m-
306 resolution raster grid (Fig. 3). The areas and TPUs of high emissions can be identified. For the
307 transport sector, high emissions were identified in the Cross-Harbour Tunnel and some major roads
308 connecting the New Territories and Kowloon. The emissions from the business sector are the
309 largest among all sectors. Commercial buildings are mainly located in Kowloon and Hong Kong
310 Island, and the high emissions in this sector are concentrated in these areas. Emissions from the
311 residential sector are relatively low but cover a large area of Hong Kong. There are few industries

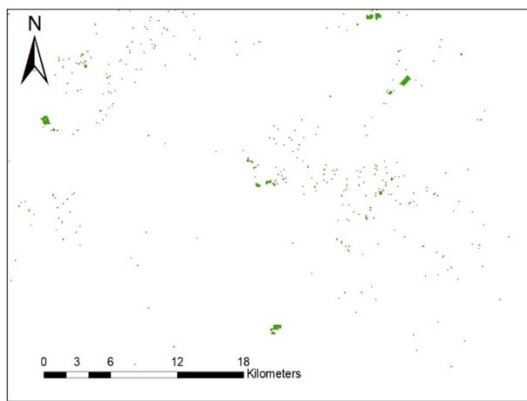
312 in Hong Kong so that the emissions from the industrial sector are not evident from the mapping
313 results. The total emissions mapping can reflect that the high-density urban areas in the central of
314 Hong Kong have higher emissions and should be taken seriously into account in the low-carbon
315 development. Also, the results are capable of identifying the variations of carbon emissions across
316 different buildings. The emissions of each TPU were summarized in Fig. 3 (f) and TPUs with high
317 emissions such as Yau Tsim Mong, Central & Western can be detected, therefore, the local
318 planners and policymakers can target these TPUs for developing low-carbon strategies.



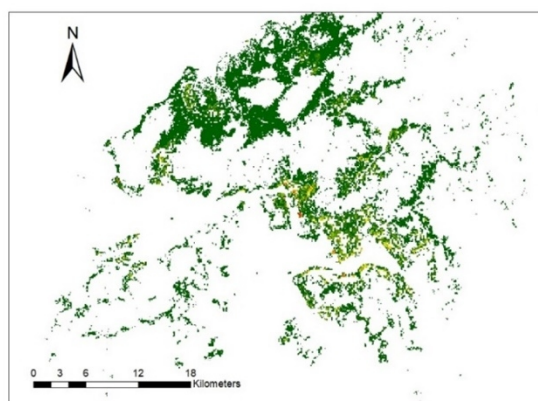
(a) Transport sector



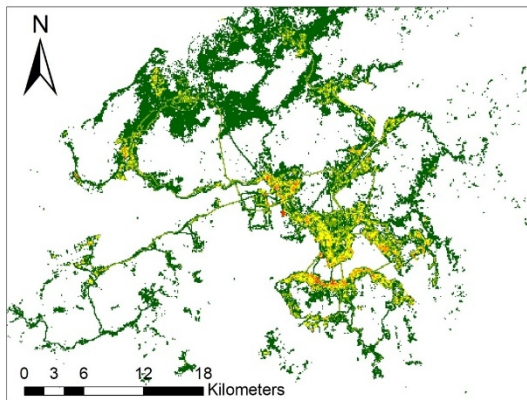
(b) Business sector



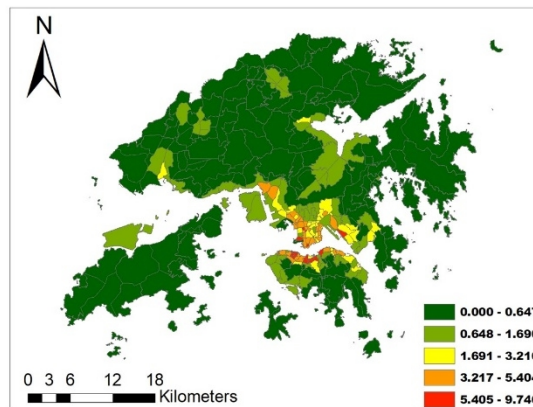
(c) Industry sector



(d) Residence sector



(e) Total emissions



(f) Total emissions by TPU

319

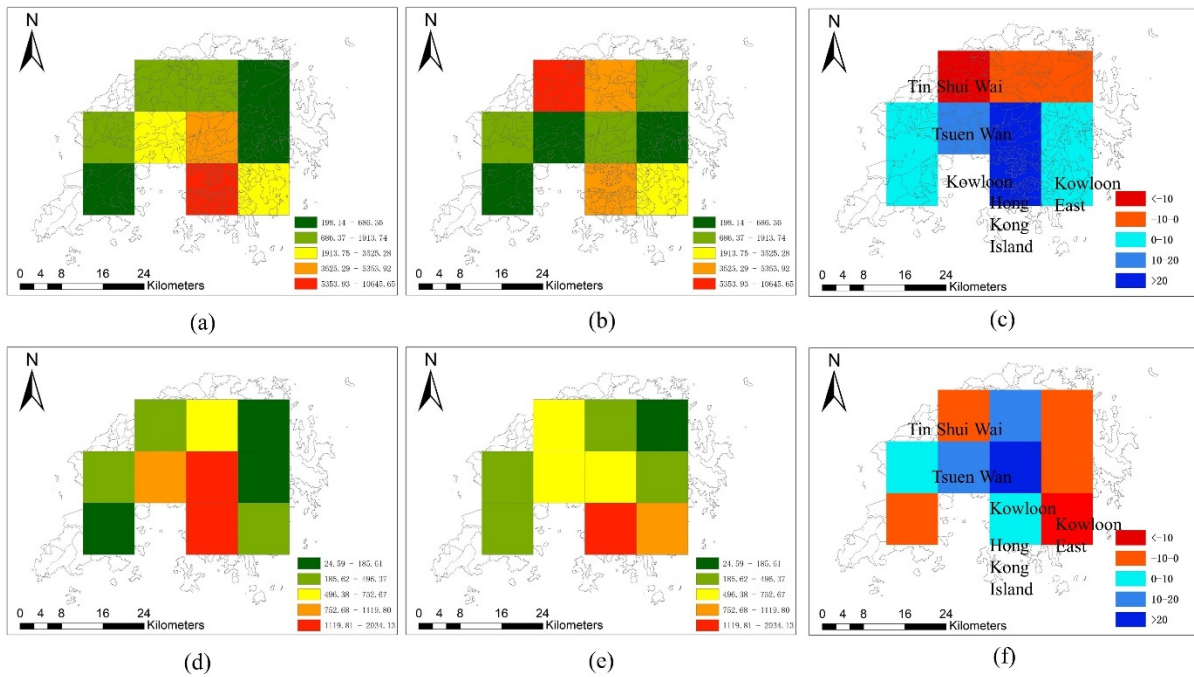
320 Fig. 3. carbon emissions in (a) transport sector, (b) business sector, (c) industry sector, (d)

321 residence industrial sector, (e) total emissions and (f) average carbon emissions in each TPU (unit:

322 Kt)

323 **3.2 Cross comparison with the EDGAR data**

324 The modelling results for Hong Kong were validated by comparing with the corresponding results
 325 from the EDGAR database [11, 47]. The EDGAR data from the building sector (1A4+1A5) and
 326 the transport sector (1A3b, and 1A3c+1A3e) were used. Only the EDGAR cells completely
 327 covering Hong Kong were chosen. Ten cells of the EDGAR dataset are available for validation in
 328 Hong Kong. The original high-resolution results were aggregated to the same spatial grid and unit
 329 of the EDGAR data for comparison (Fig. 4). Fig. 4 (a) and (b) represent the building emissions
 330 from our results and the EDGAR, respectively. Fig. 4 (d) and (e) demonstrate the transport
 331 emissions in this study and the EDGAR. Fig. 4 (c) and (f) reveal the differences between our results
 332 and the EDGAR in building and transport sector.



333
 334 Fig. 4. comparison of the results with EDGAR (a) Building emissions from this study; (b) Building
 335 emissions from EDGAR; (c) difference between (a) and (b); (d) transport emissions from this study
 336 (e) transport emissions from EDGAR; and (f) difference between (d) and (e), (unit: Kt).

337 In general, both results in the building and transport sectors reflect larger emissions in high-density
338 urban areas of Kowloon and Hong Kong Island, and smaller ones in less populated areas. EDGAR
339 reflects larger emissions in Tin Shui Wai in the northwest of Hong Kong where rural land use
340 dominates, while our proposed results demonstrate lower emissions in the same grid for the
341 building sector. The emissions in the building sector should be lower in Tin Shui Wai since there
342 are fewer population and buildings. The high emissions of the EDGAR data can result from the
343 10km spatial grid which may incorporate the emissions from the adjacent Shenzhen city. The
344 emissions in Tsuen Wan are identified higher in our results than the EDGAR. Tsuen Wan is one
345 of the densely populated old towns and famous for its old industrial areas in which still many
346 commercial activities happen, so the higher emissions from our results can better illustrate the
347 spatial pattern of the emissions of this area.

348

349 For the transport sector, our results also detected larger carbon emissions in high-density areas of
350 Tsuen Wan and Kowloon. The two districts are important transportation hubs with tunnels
351 connecting the urban area and the New Territories. There are also a large number of buses to the
352 airport in Tsuen Wan district. Therefore, it is reasonable for our results to have higher values of
353 the transport emissions in these two districts. The EDGAR has a larger emission magnitude in the
354 southeast and northwest of Hong Kong. The Kowloon East in the southeast of Hong Kong used to
355 be an industrial district and is one of the most highly populated districts in Hong Kong. The
356 emissions of the EDGAR were calculated based on population density and industrial process [48];
357 therefore, this district has a large amount of carbon emissions from the EDGAR database. However,
358 the building density in this district is relatively low in Hong Kong, and the industrial buildings are
359 mainly used as warehouses, or transformed into business or residential buildings since the 1980s

360 [49]. Thus, the current building use and building density can account for the low carbon emissions
361 in this district from the proposed model.

362

363 In sum, our results can better reveal the spatial pattern of the carbon emissions in Hong Kong in
364 both the building and the transport sectors due to the finer spatial grid and the consideration of
365 building attributes. The model shows more reasonable results especially in high-density urban
366 areas with massive commercial buildings.

367

368 **4. DISCUSSIONS**

369 **4.1 Possible application in other cities**

370 Since the spatial emission inventory tool uses open data sources and simple algorithms, it has the
371 potential to be applied in cities worldwide. There are generally four types of input data in the
372 proposed model: statistical energy consumption at the city level, building morphology, building
373 use, traffic flow. The statistical energy consumption data can be provided by the local government
374 and is openly available for most cities in the world. Indeed, some cities don't have such energy
375 use data, and they can be extracted from some global emission databases such as EDGAR. In this
376 model, the building morphology was acquired from AW3D30 and Maps static API. This building
377 morphology extraction method has global coverage and fit-for-purpose accuracy. Moreover, there
378 are also some local 3D building data sources for cities and can serve as the substitute for the
379 building morphology data.

380

381 The building use and traffic flow information adopted in this study are local datasets that may not
382 be available in other cities and they could be the major factors influencing the broad applicability

383 of the inventory tool. The building use was extracted and converted by geocoding the name list
384 and web scraping since the Hong Kong government has published detailed building name lists for
385 public buildings. However, the name list of buildings may be inaccessible, and the map service
386 may not contain sufficient building use information for other cities, which may affect the generic
387 application of this approach. The Place API from the Google maps platform can provide point of
388 interest (POI) information such as restaurants, hotels with global coverage and can be used as a
389 usable alternative for building use extraction. Therefore, the methods for building emissions
390 estimation show the possibility to be applied in other cities. Traffic flow was estimated through
391 the traffic census from counting stations which is difficult for researchers to acquire. Meanwhile,
392 there are some traffic flow estimating models using open data, such as the MATSim model, an
393 open-source framework for implementing large-scale agent-based transport simulations [50]. In
394 sum, the inventory tool has the potential of generic application and can be transferable to other
395 cities by using alternative ways to extract building use and traffic flow using open data. The present
396 study demonstrates a generalizable logic pathway of creating carbon emission spatial inventory by
397 the development of the hybrid method and the inventory tool.

398

399

400 **4.2 Limitations and possible improvements**

401 The input data adopted in the model can cause uncertainties in estimating carbon emissions (IPCC
402 2001). These uncertainties can be related the insufficient information about the emission processes,
403 measuring instruments, data quality, etc.[51, 52]. Potential uncertainties of the inventory may
404 come from emission sources and the proxy data.

405

406 The emission sources and the proxy data are all derived from open data. 3D Buildings retrieved
407 from maps static API and AW3D30 are the emission sources and the proxy data for building
408 emissions in this approach. The accuracy assessment through the linear regression between the
409 extracted buildings and the actual buildings shows that the R^2 for the buildings is around 70% and
410 72% for the BVD with 100m spatial grid [45]. The R^2 is found to increase with a coarser spatial
411 grid and can reach over 80% with 500m spatial resolution[45]. Therefore, the uncertainty from the
412 3D building can decrease with the coarser spatial grid. Moreover, there are other open building
413 data sources such as the OpenStreetMap (OSM) or remote sensing data. The OSM building data
414 has a problem in the architectural details and the completeness of the building footprints [53, 54]
415 and can also be uncertain in modelling the urban carbon emissions. The high-quality remote
416 sensing data such as Sentinel-1 SAR data has finer spatial resolution than the AW3D30 and can
417 be used to replace the AW3D30 in the extraction of the building height to reduce the uncertainty
418 from the building.

419
420 Moreover, there are many commercial mixed-use residential buildings in Hong Kong. This study
421 regards this kind of mixed-use buildings as residential use due to data availability. Residential
422 building use is the dominant function of such building and mixed-use land use mode is less
423 common in other cities than in high-density cities like Hong Kong. Therefore, the uncertainty of
424 the mixed-use will not affect the generic application of this approach.

425
426 Building heating and cooling energy demand can vary greatly in different seasons and years. This
427 study was conducted for the year 2016 to acquire the annual emissions maps. Since the major aim
428 of this pilot study is to demonstrate the workflow, the seasonal and the inter-year variations are

429 not accounted for by the present study. The present study provides an annual result as a
430 demonstration of how the newly developed hybrid method is used. The method itself is readily
431 applicable for other years or periods of interest as long as we feed the inventory tool with statistical
432 energy data of the corresponding period. Future work has been planned to apply the tool for
433 understanding the seasonal and inter-year variations of the carbon emissions.

434
435 Finally, since the lack of real emission data for verification is currently still a worldwide issue in
436 most parts of the world, the results can only be validated through cross-comparison with other
437 emission inventories such as GCP, EDGAR. In the future, other real measure instruments will be
438 adopted to achieve a more reliable accuracy assessment.

439

440

441 **4.3 Implications for low-carbon city management**

442 In Hong Kong, buildings account for about 90% of the electricity used and over 60% of the carbon
443 emission [55]. The buildings are the major focus of low-carbon development and energy saving
444 for the local government [39]. Since our developed spatial-inventory tool adopts precise building
445 information, it is found that those hotspot areas of urban carbon emissions are located in downtown
446 areas with very high building density. This study results would provide Hong Kong local
447 government with useful information to manage the energy consumption of buildings and make an
448 energy reduction strategy at the district level accordingly, such as developing a district cooling
449 system, adopting renewable energy resources at different districts. This study results could also be
450 used to have a comprehensive understanding of the relationship between the cooling energy
451 requirement and building emissions.

452

453 **5. CONCLUSION**

454 In this study, a method for creating urban carbon emissions inventory at a high-resolution was
455 developed by incorporating open urban form data. We demonstrated that the approach can be
456 applied in high-density Hong Kong. The emissions from transportation and buildings were
457 generated for entire Hong Kong at both a 100m-resolution grid and the TPU level in 2016. The
458 hotspot areas and TPUs of high emissions were identified. Validation results show that the method
459 has reasonably represented both the total emissions and the spatial pattern of urban carbon
460 emissions of Hong Kong.

461

462 The modelling method using open urban form data can more accurately model the spatial pattern
463 of the urban carbon emissions and can be transferable to other cities, therefore contributing to the
464 global collaborative effort in urban carbon emission mitigation. The spatial inventory tool can help
465 support policy decisions regarding urban energy resilience and low-carbon development for
466 different cities. Moreover, it can provide useful information for policymakers of C40 cities that
467 aims to tackle climate change reduce GHG emissions to determine which areas should be targeted
468 to conduct relevant action for improving energy efficiency and carbon emissions mitigation. The
469 map can offer the policymakers with information on buildings and sectors responsible for high
470 emissions, in particular, the variations of the emissions across different buildings. For example, in
471 Hong Kong, with such maps, it would be easier for local government officials to identify those
472 hotspot areas of carbon emission so they could implement energy efficiency ordinance accordingly.

473

474 There are also limitations of this study. The uncertainties from the proxy data and emission source
475 can affect the accuracy of the modelling. High-quality building data can be helpful to improve the

476 modelling results. We plan to reduce the above uncertainties by using other high-quality building
477 data in future work. Also, the hourly variation of carbon emissions can reflect the carbon emissions
478 in more detail for better informing the low-carbon development. The hourly variation of the carbon
479 emissions can be modelled in future studies by using popular times of Google Maps API for the
480 building sector, and GPS and machine learning technique for the transport sector.

481

482 **ACKNOWLEDGEMENT**

483 The study is supported by a PGS studentship from The Chinese University of Hong Kong. It is
484 also partially supported by the Strategic Interdisciplinary Research Scheme of The University of
485 Hong Kong.

486

487

488

489 **REFERENCES**

- 490 1. IPCC, *IPCC, 2014: climate change 2014: synthesis report. Contribution of Working Groups I II and*
491 *III to the Fifth Assessment Report of the intergovernmental panel on Climate Change*. IPCC,
492 Geneva, Switzerland, 2014. **151**.
- 493 2. IPCC, *the Fourth Assessment Report (AR4) of the United Nations Intergovernmental Panel on*
494 *Climate Change (IPCC)*. Millenium Ecosystem Assessment. Tillgänglig på [www.](http://www.millenniumassessment.org)
495 [millenniumassessment.org](http://www.millenniumassessment.org), 2007.
- 496 3. Sugahara, M. and L. Bermont, *Energy and resilient cities*. 2016.
- 497 4. International Energy Agency, *Energy Technology Perspectives 2016: Towards Sustainable Urban*
498 *Energy Systems*2016: OECD.
- 499 5. UN DESA, *World Urbanisation Prospects, 2018 Revision*, 2018: New York.
- 500 6. Yang, F., Y. Li, and J. Xu, *Review on Urban GHG Inventory in China*. International Review for
501 Spatial Planning and Sustainable Development, 2016. **4**(2): p. 46-59.
- 502 7. Bai, X., et al., *Six research priorities for cities and climate change*, 2018, Nature Publishing Group.
- 503 8. WANG, J., et al., *China 10km carbon dioxide emissions grid dataset and spatial characteristic*
504 *analysis*. China Environmental Science, 2014. **31**(1): p. 1-6.
- 505 9. Cai, B., et al., *Source data supported high resolution carbon emissions inventory for urban areas*
506 *of the Beijing-Tianjin-Hebei region: Spatial patterns, decomposition and policy implications*. J
507 Environ Manage, 2018. **206**: p. 786-799.

- 508 10. Cai, B., et al., *China high resolution emission database (CHRED) with point emission sources,*
509 *gridded emission data, and supplementary socioeconomic data.* Resources, Conservation and
510 Recycling, 2018. **129**: p. 232-239.
- 511 11. Olivier, J.G., et al., *Description of EDGAR Version 2.0: A set of global emission inventories of*
512 *greenhouse gases and ozone-depleting substances for all anthropogenic and most natural*
513 *sources on a per country basis and on 1 degree x 1 degree grid.* 1996.
- 514 12. Gurney, K.R., et al., *High resolution fossil fuel combustion CO2 emission fluxes for the United*
515 *States.* Environ Sci Technol, 2009. **43**(14): p. 5535-5541.
- 516 13. Wu, Y., et al., *Mapping building carbon emissions within local climate zones in Shanghai.* Energy
517 Procedia, 2018. **152**: p. 815-822.
- 518 14. Cai, B. and L. Zhang, *Study on the Spatial Characteristics of Urban CO2 Emissions in Shanghai.*
519 PROGRESSUS INQUISITIONES DE MUTATIONE CLIMATIS, 2014. **10**(6): p. 417-426.
- 520 15. Sharifi, A., et al., *Urban carbon mapping: Towards a standardized framework.* Energy Procedia
521 2018. **152**: p. 799-808.
- 522 16. Jing, Q., et al., *A top-bottom method for city-scale energy-related CO2 emissions estimation: A*
523 *case study of 41 Chinese cities.* Journal of Cleaner Production, 2018. **202**: p. 444-455.
- 524 17. Han, J., et al., *An improved nightlight-based method for modeling urban CO 2 emissions.*
525 Environmental Modelling & Software, 2018. **107**: p. 307-320.
- 526 18. Xie, Y. and Q. Weng, *Detecting urban-scale dynamics of electricity consumption at Chinese cities*
527 *using time-series DMSP-OLS (Defense Meteorological Satellite Program-Operational Linescan*
528 *System) nighttime light imageries.* Energy, 2016. **100**: p. 177-189.
- 529 19. Wang, Y. and G. Li, *Mapping urban CO2 emissions using DMSP/OLS 'city lights' satellite data in*
530 *China.* Environment and Planning A: Economy and Space, 2016. **49**(2): p. 248-251.
- 531 20. Shi, K., et al., *Modeling spatiotemporal CO2 (carbon dioxide) emission dynamics in China from*
532 *DMSP-OLS nighttime stable light data using panel data analysis.* Applied Energy, 2016. **168**: p.
533 523-533.
- 534 21. Meng, L., et al., *Estimating CO2 (carbon dioxide) emissions at urban scales by DMSP/OLS*
535 *(Defense Meteorological Satellite Program's Operational Linescan System) nighttime light*
536 *imagery: Methodological challenges and a case study for China.* Energy, 2014. **71**: p. 468-478.
- 537 22. Zhuo, L., et al., *An improved method of night-time light saturation reduction based on EVI.*
538 International Journal of Remote Sensing, 2015. **36**(16): p. 4114-4130.
- 539 23. Elvidge, C.D., et al., *Why VIIRS data are superior to DMSP for mapping nighttime lights.*
540 Proceedings of the Asia-Pacific Advanced Network, 2013. **35**(0): p. 62.
- 541 24. Ghosh, T., et al., *Creating a Global Grid of Distributed Fossil Fuel CO2 Emissions from Nighttime*
542 *Satellite Imagery.* Energies, 2010. **3**(12): p. 1895-1913.
- 543 25. Oda, T. and S. Maksyutov, *A very high-resolution global fossil fuel CO 2 emission inventory*
544 *derived using a point source database and satellite observations of nighttime lights, 1980–2007.*
545 Atmospheric Chemistry and Physics Discussions, 2010. **10**(7): p. 16307-16344.
- 546 26. Christen, A., et al., *A LiDAR-based urban metabolism approach to neighbourhood scale energy*
547 *and carbon emissions modelling,* 2010, University of British Columbia.
- 548 27. Li, D.H., L. Yang, and J.C. Lam, *Impact of climate change on energy use in the built environment in*
549 *different climate zones—a review.* Energy, 2012. **42**(1): p. 103-112.
- 550 28. Cai, M., et al., *A review of spatial modelling studies on urban carbon emissions in China (under*
551 *review).* Renewable and Sustainable Energy Reviews, 2020.
- 552 29. Makido, Y., Y. Yamagata, and S. Dhakal, *EFFECT OF URBAN FORMS: TOWARDS THE REDUCTION*
553 *OF CO2 EMISSIONS,* in ASPRS 2010 Annual Conference 2010: San Diego, California.
- 554 30. Ma, J., Z. Liu, and Y. Chai, *The impact of urban form on CO2 emission from work and non-work*
555 *trips: The case of Beijing, China.* Habitat International, 2015. **47**: p. 1-10.

- 556 31. Fang, C., S. Wang, and G. Li, *Changing urban forms and carbon dioxide emissions in China: A case*
557 *study of 30 provincial capital cities*. Applied Energy, 2015. **158**: p. 519-531.
- 558 32. Ibrahim, N., et al., *Greenhouse gas emissions from cities: comparison of international inventory*
559 *frameworks*. Local Environment, 2012. **17**(2): p. 223-241.
- 560 33. Cai, B., *Characteristics analysis of CO₂ emissions of cities in China: Based on 0.1 degree grid*
561 *dataset*. China Population, Resources and Environment, 2012. **22**: p. 151-157.
- 562 34. Wang, J., et al., *High resolution carbon dioxide emission gridded data for China derived from*
563 *point sources*. Environ Sci Technol, 2014. **48**(12): p. 7085-93.
- 564 35. Environmental Protection Department of Hong Kong, *Hong Kong greenhouse gas inventory for*
565 *2016 released*, 2018: Hong Kong.
- 566 36. Census and Statistics Department of Hong Kong, *Population and Household Statistics Analysed*
567 *by District Council District*, 2018.
- 568 37. Electrical & Mechanical Services Department of Hong Kong, *Hong Kong Energy End-use Data*
569 *2018*, 2018: Hong Kong.
- 570 38. Environment Bureau of Hong Kong, *Hong Kong's Climate Action Plan 2030+*, 2017: Hong Kong.
- 571 39. Environment Bureau of Hong Kong, *Hong Kong Climate Change Report 2015*, 2015: Hong Kong.
- 572 40. Xu, Y., et al., *Urban morphology detection and computation for urban climate research*.
573 *Landscape and Urban Planning*, 2017. **167**: p. 212-224.
- 574 41. Census and Statistics Department of Hong Kong, *Hong Kong Energy Statistics Annual Report*
575 *(2016 Edition)*, 2017: Hong Kong.
- 576 42. IPCC, *2006 IPCC guidelines for national greenhouse gas inventories*2006: Intergovernmental
577 Panel on Climate Change.
- 578 43. Civil Aviation Department, *Civil Aviation Department Environmental Report 2016*, 2016: Hong
579 Kong.
- 580 44. Transport Department, *The Annual Traffic Census*, 2019: Hong Kong.
- 581 45. Ren, C., et al., *Developing a rapid method for 3-dimensional urban morphology extraction using*
582 *open-source data* Sustainable Cities and Society, 2019.
- 583 46. Xia, L. and Y. Shao, *Modelling of traffic flow and air pollution emission with application to Hong*
584 *Kong Island*. Environmental Modelling & Software, 2005. **20**(9): p. 1175-1188.
- 585 47. Crippa, M.S., E.; Huang, G.; Guizzardi, D.; Koffi, E.; Muntean, M.; Schieberle, C.; Friedrich, R.;
586 Janssens-Maenhout, G., *High resolution temporal profiles in the Emissions Database for Global*
587 *Atmospheric Research (EDGAR)*. Nature Scientific Data, 2019. **submitted**.
- 588 48. Pesaresi, M. and S. Freire, *GHS Settlement grid following the REGIO model 2014 in application to*
589 *GHSL Landsat and CIESIN GPW v4-multitemporal (1975-1990-2000-2015)*. European
590 Commission, Joint Research Centre, JRC Data Catalogue, 2016.
- 591 49. Cheng, W.-l., *Kowloon East then and now: transformation of the former*. 2015.
- 592 50. W Axhausen, K., A. Horni, and K. Nagel, *The multi-agent transport simulation MATSim*2016:
593 Ubiquity Press.
- 594 51. White, T., et al., *Greenhouse gas inventories: dealing with uncertainty*2011: Springer Science &
595 Business Media.
- 596 52. Ometto, J.P., et al., *Uncertainties in Greenhouse Gas Inventories: Expanding Our*
597 *Perspective*2015: Springer.
- 598 53. Hecht, R., C. Kunze, and S. Hahmann, *Measuring completeness of building footprints in*
599 *OpenStreetMap over space and time*. ISPRS International Journal of Geo-Information, 2013. **2**(4):
600 p. 1066-1091.
- 601 54. Fan, H., et al., *Quality assessment for building footprints data on OpenStreetMap*. International
602 *Journal of Geographical Information Science*, 2014. **28**(4): p. 700-719.

603 55. Environment Bureau of Hong Kong, *Deepening Energy Saving in Existing Buildings in Hong Kong*
604 *through '4Ts' partnership*, 2017: Hong Kong.
605
606